

Experimental Validation of Time-Synchronized Operations for Software-Defined Elastic Optical Networks

Original

Experimental Validation of Time-Synchronized Operations for Software-Defined Elastic Optical Networks / Bravalheri, Anderson; GARRICH ALABARCE, Miquel; Muqaddas, ABUBAKAR SIDDIQUE; Giaccone, Paolo; Bianco, Andrea. - In: JOURNAL OF OPTICAL COMMUNICATIONS AND NETWORKING. - ISSN 1943-0620. - STAMPA. - 10:1(2018), pp. 51-59. [10.1364/JOCN.10.000A51]

Availability:

This version is available at: 11583/2688805 since: 2018-04-14T07:59:38Z

Publisher:

IEEE/OSA

Published

DOI:10.1364/JOCN.10.000A51

Terms of use:

This article is made available under terms and conditions as specified in the corresponding bibliographic description in the repository

Publisher copyright

IEEE postprint/Author's Accepted Manuscript

©2018 IEEE. Personal use of this material is permitted. Permission from IEEE must be obtained for all other uses, in any current or future media, including reprinting/republishing this material for advertising or promotional purposes, creating new collecting works, for resale or lists, or reuse of any copyrighted component of this work in other works.

(Article begins on next page)

Experimental Validation of Time-Synchronized Operations for Software-defined Elastic Optical Networks

Anderson Bravalheri, Miquel Garrich A., Abubakar Siddique Muqaddas, Paolo Giaccone and Andrea Bianco

Abstract—Elastic Optical Networks (EON) have been proposed as a solution to efficiently exploit the spectrum resources in the physical layer of optical networks. Moreover, by centralizing legacy Generalized Multi-Protocol Label Switching (GMPLS) control-plane functionalities and providing a global network view, Software Defined Networking (SDN) enables advanced network programmability valuable to control and configure the technological breakthroughs of EON. In this paper, we review our recent proposal [1] of time-synchronized operations (TSO) to minimize disruption time during lightpath reassignment in EON. TSO have been recently standardized in SDN and here we discuss its implementation using NETCONF and OpenFlow in optical networks. Subsequently, we update our analytical model considering an experimental characterization of the WSS operation time. Then, we extend our previous work with an experimental validation of TSO for lightpath reassignment in a five-node metropolitan optical network test-bed. Results validate the convenience of our TSO-based approach against a traditional asynchronous technique given its reduction of disruption time while both techniques maintain a similar network performance in terms of optical signal-to-noise ratio (OSNR) and optical power budget.

Index Terms—Elastic optical networks; Software defined networks; Time-synchronized operations.

I. INTRODUCTION

TRAFFIC volumes in carrier networks keep growing dramatically, driven by the proliferation of high-bandwidth services and applications. To address this challenge, Elastic Optical Networking (EON) enables an efficient use of spectrum resources valuable to extend the lifetime of already deployed optical fibers [2]. EON performs flexible frequency allocation in the network using reconfigurable optical add/drop multiplexers (ROADMs) [3] and bandwidth-variable transmission techniques [4]. In particular, EONs use the spectrum resources of the data plane following the guidelines reported in the ITU-T Recommendation G.694.1 from 2012 [5]. However, the migration from classical wavelength division multiplexed (WDM) fixed-grid spectrum allocation towards flexible EON may require notable long-term investments [6] or gradual migration of the wavelength selective switch (WSS) equipment [7]. Moreover, telecom operators face operational chal-

lenges in order to manage such a diverse multi-technology scenario which may also include multi-vendor equipment interoperability issues [8]. In more detail, [8] reports a demonstration of interoperability between multi-vendor optical equipment with the need to adapt several interfaces just to perform an experimental end-to-end resource provisioning. Indeed, these operational challenges may endanger the potential deployment of next-generation flexible-rate transponders and EONs [9].

To address these challenges, novel Software Defined Networking (SDN) approaches [10] enable advanced control and configuration features suitable for the breakthrough technologies of the EON data plane. Although legacy Generalized Multi-Protocol Label Switching (GMPLS) / Path Computation Element (PCE) architectures already offered a fully separated control plane from the control plane, SDN enhances network programmability via open programmatic interfaces, reduces vendor lock-in issues, and permits innovation and evolution of the network infrastructure [11]. In particular, academic initiatives to control optical components recently proposed open YANG models [12] for EON [13]. In this research direction, YANG models have been proposed for monitoring functionalities in EONs [14] and specific models to manage sliceable transponders [15]. More recently, specific NETCONF protocol features and YANG models have also been proposed to address optical network failure issues [16]. On the industrial side, the recent OpenROADM standardization initiative [17], proposes an interface for multi-vendor ROADM access and configuration based on YANG models. More specifically, OpenROADM targets the disaggregation of traditionally proprietary ROADM systems and SDN-enablement of traditionally fixed ROADMs.

In the EON data plane, routing and spectrum assignment (RSA) schemes allocate lightpaths ensuring that a set of frequency slots (FS) are *continuous* throughout the routing path [18]. Connections in EON are established (and removed) dynamically, thus potentially leaving sparse FS that become difficult to use by the RSA to reduce blocking probability. This fragmentation problem has been recently addressed with hitless defragmentation techniques able to reallocate the light-path frequencies without traffic disruption. Examples are the push-pull technique [19], which allows spectrum retuning only over contiguous vacant FS from the source to the destination frequency; and the hop-retuning technique [20], which strictly requires a number of photodetectors equal to the number of FS. Due to system complexity, the former technique is usually preferred over the latter. However, even with RSA schemes combined with push-pull [21], high-load scenarios may drive

A. Bravalheri (email: abraval@cpqd.com.br) is with CPqD, rua Dr. Ricardo Benetton Martins, s/n, 13086-902, Campinas, SP, Brazil.

M. Garrich A. is with the Department of Electronics and Telecommunications Engineering, Politecnico di Torino, Torino, Italy, and with CPqD.

A. S. Muqaddas, A. Bianco and P. Giaccone are with the Department of Electronics and Telecommunications Engineering, Politecnico di Torino, Torino, Italy.

the network towards the so called “end-of-line situations” limiting the potential benefits of EON [22]. *End-of-line* situations are defined by [22] as cases in which a lightpath obstructs push-pull spectrum defragmentation or non-continuous vacant FS contribute to network blocking. These situations require lightpath rerouting to exploit the remaining capacity not being used by existing RSA and defragmentation techniques, albeit in a non hitless manner.

In this context, SDN could be exploited to address this challenge. In particular, time-synchronized operations (TSO), have been recently proposed in the form of southbound protocol extensions to coordinate distributed operations simultaneously [23]. Indeed, TSO are gaining interest in the research community as an SDN feature capable to improve network performance [24] and to develop novel applications [25].

In this paper, we review our recent proposal [1] of TSO for EON to address end-of-line situations efficiently performing lightpath rerouting to minimize the disruption time. We discuss the implementation of our proposal using the existing protocols, and we show the benefits in a test scenario comparing performance against traditional asynchronous operations.

The novel contribution with respect to [1] is an experimental validation of TSO for lightpath reassignment in a five-node metropolitan optical network test-bed. We compare the network performance in terms of optical signal-to-noise ratio (OSNR) and optical power budget between our TSO-based approach and the traditional asynchronous technique. We observe that both techniques maintain a similar network performance, thus validating the convenience of the TSO-based approach given its reduction of disruption time.

II. AN END-OF-LINE SCENARIO: NON-CONTINUOUS VACANT FS

In this section, we provide an example of end-of-line situation to illustrate the need for lightpath rerouting to better exploit the remaining optical spectrum resources. Then, we detail the traditional asynchronous technique commonly employed in non SDN-enabled networks to address these situations

Fig. 1 shows an example of end-of-line situation due to non-continuous vacant FS in a network assuming 6 FS per link. The numbers in the spectrum indicate the number of allocated FS. Initially, assume that there are 4 lightpaths in the network. Thus 1 FS is available in both $A-B-D$ and $A-C-D$ paths. Let us assume a new lightpath requests 2 FS from A to D . Note that defragmentation would not increase the available FS in each link to accommodate this new lightpath. Therefore, either this new request is rejected or existing lightpaths need to be rerouted. The latter case is preferred, as shown in Fig. 2, because it reduces the network blocking probability. Rerouting in Fig. 1 requires swapping lightpaths to achieve the configuration in Fig. 2.

We define as *asynchronous* (ASY) approach the technique that executes the operations asynchronously as depicted in Fig. 3a. The ASY approach addresses the end-of-line situation shown in Fig. 1 to achieve the network state in Fig. 2 performing the following four operations. First, L_3 is disrupted sending *tear-down* requests to all the nodes. Second, L_1 is

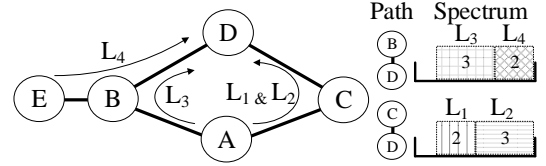


Fig. 1: Topology with lightpaths in an end-of-line scenario

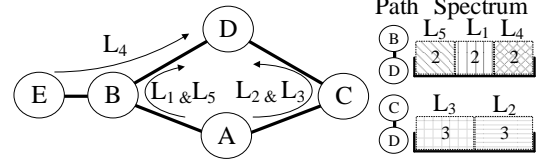


Fig. 2: Re-routing to accommodate a new lightpath

rerouted from $A-C-D$ to $A-B-D$ with two commands *tear-down* and *setup* for its migration. Third, L_3 is now *setup* in its new route $A-C-D$. Finally, the new lightpath L_5 can be allocated on $A-B-D$ and the network state depicted in Fig. 2 is achieved. Note that this operation of lightpath swapping implies a non-negligible disruption time for L_3 . Nonetheless, it worthwhile mentioning that differently from the sequence illustrated in Fig. 3a, the reassignment of L_1 could be performed without any disruption time just by implementing Make-before-Break (MbB) technique as specified in RSVP-TE [26]. In particular, given that spectrum resources are made available using overprovisioning in the $A-C-D$ path by tearing down L_3 , L_1 can be setup in this new route before tearing down its initial allocation in $A-B-D$. However, note that MbB for L_1 does not reduce the disruption time for L_3 .

III. TIME-SYNCHRONIZED OPERATIONS FOR EON

In this section, we review our recent proposal [1] of time-synchronized operations (TSO) for EON which leverage on recently provided features in SDN. Simultaneous operations can be coordinated using timestamps within industry-standard southbound configuration messages. In the case of lightpath swapping, our approach operates as shown in Figs. 3b and 3c.

In case of NETCONF, time extensions to the protocol have been recently published as an RFC [27]. The SDN controller sends a *scheduled-RPC* message to the optical node to execute an operation at a specific time. Note that NETCONF does not provide the capability to bundle operations natively. Therefore, one command per operation is issued and scheduled using timestamps in a sequential manner accounting for the configuration time as shown in Fig. 3b (i.e. four operations same as ASY). We refer to this implementation as Native-NETCONF (N-NC). Indeed, similarly as for the ASY case, the commands required to reroute L_1 could be inverted (i.e., setup before tear down) implementing the MbB approach so that L_1 does not experience any disruption time. Nonetheless, an Intelligent Agent can be implemented either at the SDN controller or at the optical node that processes NETCONF (IA-NC) messages to group several operations into a single configuration [28].

In case of OpenFlow (OF), two features are included in its latest version 1.5 [29]: a *bundle* of operations can be executed

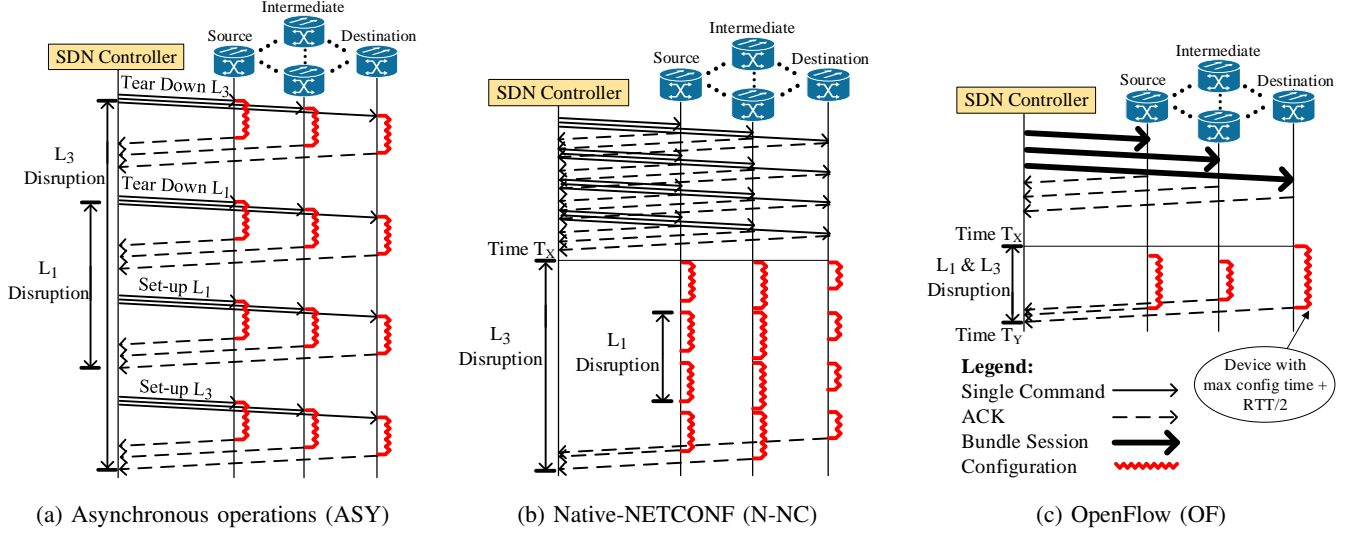


Fig. 3: Asynchronous vs. TSO-based approaches in NETCONF and OpenFlow. Source node corresponds to A, intermediate nodes correspond to B and C, and destination node corresponds to D, respectively, in Figs. 1 and 2.

simultaneously [10], and this bundle can be *scheduled* for execution at a given time, as shown in Fig. 3c. The scheduling of the bundle depends on the node with the maximum sum of the configuration time plus the half round trip time (RTT). In Fig. 3c, we assume that this is the case of the destination node and it starts to execute the bundle of operations at time T_X and it acknowledges the SDN controller at time T_Y after it finishes its configuration. Given that all other nodes have a configuration time smaller than the destination node, their configuration can be done within the time interval between T_X and T_Y . By doing so, the smaller configuration times in other nodes compared to the maximum case (destination node in Fig. 3(c)) become transparent to the disruption time. Indeed, this relaxes the requirement of full time-synchronization for the OF approach. Bundling commands in OF requires opening a session by the SDN controller to the optical node with a *bundle-open* message. Thereafter, multiple commands are sent to the optical node to be added to the bundle. This is followed by a *bundle-commit* message to specify the time at which the bundle should be executed. Note that bundling network operations by means of the OF bundling feature differs from launching an application (e.g., script file or program) at the SDN controller that issues multiple commands to a given network node. For instance, multiple WSS configurations for different spectrum filtering patterns could be merged into a single WSS filtering pattern modification within a bundle. However, the approach using the multiple-command application would update the WSS filtering pattern upon receiving each command separately. It is worthwhile mentioning that OF and IA-NC cause the same disruption as both implementations permit to bundle several operations as a single configuration. Hence, we refer to them as OF/IA-NC while evaluating their performance.

The temporal accuracy of the time-synchronized approach depends on the maximum value of two contributions. On the one hand, we consider the *worst-case configuration time* of

all optical nodes involved in the reconfiguration. This time depends on several factors including the common coexistence of data-plane devices from different vendors in carrier-grade optical networks, the dependence of the configuration time on current load of the agent at the optical node, aging issues or other random behaviors. However, this worst-case configuration time can be estimated with some error considering the average reconfiguration time with respect to the load (see Fig. 4(b)). On the other hand, *worst-case synchronization error* among devices needs to be taken into account. To this end, local clocks at the optical nodes can be synchronized with a reference clock using Precision Time Protocol (PTP), or an improved version named ReversePTP [30]. Indeed, given the accuracy of up to $1 \mu\text{s}$ provided by ReversePTP makes its contribution to the TSO inaccuracy negligible compared to optical configuration times which are in the order of seconds.

In summary, the efficiency of the TSO approach improves with better time accuracy and better knowledge of the reconfiguration time. In this work, given that all the schemes under analysis (ASY, N-NC, OF) are affected by these worst-case considerations, the current conclusions hold. Consequently, we leave further analyses on these two problems outside the scope of our work.

IV. ANALYTICAL EVALUATION OF TSO

In this section, we evaluate the disruption time of ASY, N-NC and OF/IA-NC, considering the lightpath swapping scenario of Sec. II.

We assume that each node i has a constant configuration time c_i regardless of the operation. The ASY approach is composed of four operations: tear down L_3 , tear down L_1 , setup L_1 and setup L_3 . Each operation lasts for $t_{op} = \max_i(RTT_i + c_i)$, where RTT_i is the Round Trip Time between the SDN controller and node i . Thus, the total disruption time experienced by lightpath L_3 is $t_{ASY} = 4 \times t_{op} - \min_i(RTT_i/2)$, where the second term is subtracted because the disruption starts when

the nearest node receives the tear-down message from the controller. The N-NC approach concatenates four operations, similar to ASY. Hence, the disruption time is $t_{N-NC} = 3 \max_i(c_i) + \max_i(c_i + RTT_i/2)$, where the second term is due to the last operation in which the controller receives an ACK. The OF/IA-NC permits simultaneous operations, thus the disruption lasts for $t_{OF/IA-NC} = \max_i(c_i + RTT_i/2)$.

In order to evaluate the impact of the configuration time of the WSS devices on the lightpath disruption time, we review our recently reported experimental results [28], [31]. In particular, a SDN controller makes use of a standard protocol (e.g., a REST interface) to communicate with the firmware of the WSS (Fig. 4(a)). Leveraging on YANG models, the SDN controller can issue specific requests to the firmware of the WSS. For example, the attenuation of any given WSS device at any desirable position of the optical spectrum can be arbitrarily set by the controller. Fig. 4(b) reports the time that is required to perform a change of attenuation in the WSS device as a function of the number of wavelengths for which the attenuation is being adjusted. More specifically, the empty squares report the time requirement as specified by the WSS device manufacturer. The solid squares report the time required to complete the operation inclusive of the control signaling, the firmware execution time and the WSS operation. (The signaling propagation time between the SDN controller and the optical node is negligible.) During the experiment, the applied attenuation for a given group of wavelengths is changed from maximum to minimum and vice versa. The number of wavelengths being switched is varied. Results reported in Fig. 4(b) are the average of ten experiments in two WSS devices and exhibit a linear dependence on the number of channels to be configured with minimal standard deviation (confidence intervals using vertical lines are not reported for the sake of legibility) as in [31]. The curve indicates that the time required to complete the adjustment of the WSS-applied attenuation is proportional to the number of wavelengths for which the attenuation is being adjusted.

Considering the above reported experimental results that

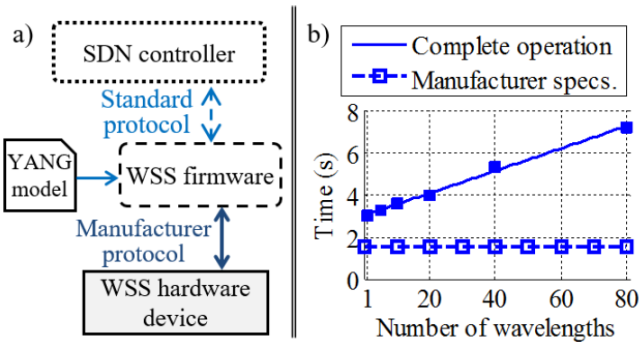


Fig. 4: (a) System modules for WSS control in the optical network test-bed. (b) Time required for a single WSS operation vs. the number of wavelengths. Empty squares report manufacturer specifications (upper bound for the WSS hardware configuration time) and solid squares report experimental measurements of a complete operation cycle, i.e., service time (average of ten experiments in two WSS devices)[28], [31].

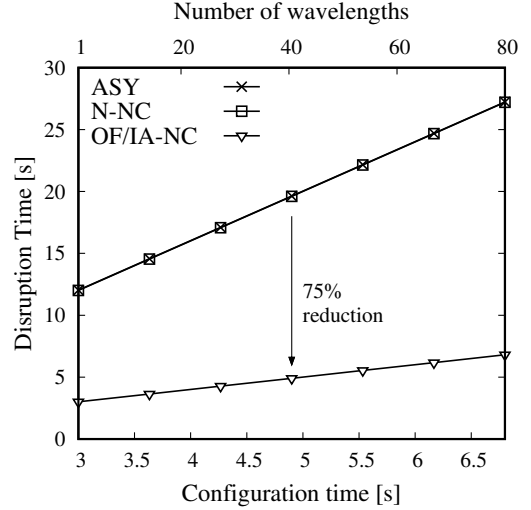


Fig. 5: Disruption time for variable number of wavelengths with $RTT = 10$ ms

characterize the WSS operation time, Fig. 5 shows the disruption time as a function of $\max_i(c_i) \in [3, 7]$ and number of wavelengths $\in [1, 80]$ with constant RTT . Note that the proportional dependence between the configuration time required by a WSS and the number of wavelengths it is required to adjust permits the double x-axis depicted in Fig. 5. OF and IA-NC outperform ASY and N-NC as they bundle all the operations in a single configuration instead of four, thus reducing the disruption time by 75%.

Finally, Fig. 6 explores the disruption time for a constant $c_i = 50$ ms, $\forall i$, small enough to observe the impact of the $\max_i(RTT_i)$. Note that a $c_i = 50$ ms is consistent with Microelectromechanical systems (MEMS) technology employed in fiber switches [32]. As in the previous analysis, the bundling feature in OF and IA-NC reduces the communication rounds between the optical nodes and the controller, thus reducing the disruption time due to RTT . Consequently, as RTT increases, the reduction grows from 75% to 83.3% when comparing OF and IA-NC against ASY. Furthermore in this case, N-NC performs better than ASY but worse than OF/IA-NC.

V. EXPERIMENTAL VALIDATION OF TSO

In this section, we first provide an overview of the five-node metropolitan optical network test-bed where the experiments are performed. Then, we detail the experimental setup that emulates the end-of-line scenario shown in Fig. 1. Finally, we report and discuss the experimental results.

A. Optical network test-bed overview

The experimental results of this work are obtained using an SDN-enabled five-node metropolitan optical network test-bed located at CPqD [28]. More specifically, the network test-bed comprises 4 ROADMs of degree 3 and a central ROADM of degree 4 interconnected to form a partial mesh topology using 100-km single mode fiber (SMF) links as shown in Fig. 7. The ROADM nodes architecture is broadcast-and-select (B&S) using one splitter per input port and one WSS per output port.

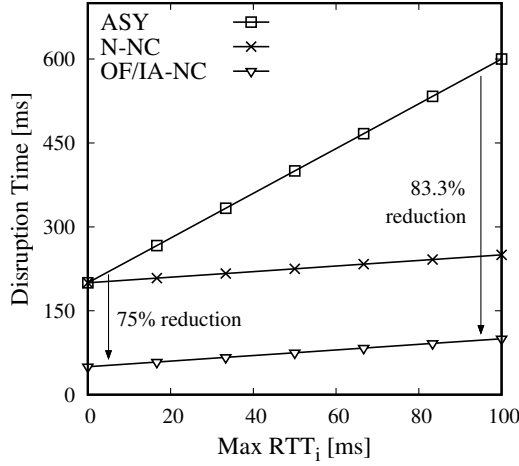


Fig. 6: Disruption time for two different scenarios

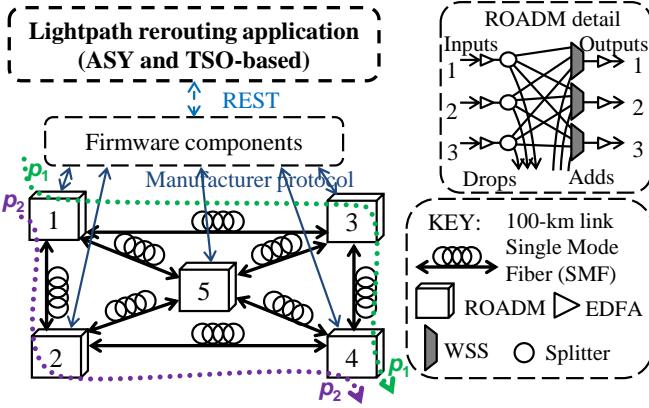


Fig. 7: General architecture for the SDN-enabled test-bed.

In particular, The WSS devices are from Finisar and belong to its ROADMs & Wavelength Management product portfolio. More specifically, 1×5 Flexgrid® WSSs¹ acquired in 2010 are used in the central ROADM, whereas 1×4 Flexgrid® WSSs² acquired in 2012 are used in the ROADMs at the edges of the network. EDFAs are placed at each input and output port to compensate for span and node losses. No physical dispersion compensation modules are used. The transmitter is composed of 80 continuous wave (CW) lasers with 50 GHz channel spacing. Each CW is modulated by four multiplexed lines of 32 Gb/s (PRBS $2^{31} - 1$), obtaining 80 128-Gb/s DP-QPSK orthogonal channels. Transmission impairments and non-linear effects are assumed to be compensated at the receiver (out of the scope of this work).

B. Experimental setup

In order to investigate the approaches described in Sections II and III for introducing new connections in an end-of-line situation, two experimental tests are carried out using

¹Product Code: 10WSPA05ZZL. Discontinued product. Preliminary version of the current 1×9 and 1×20 WSS devices detailed in <https://www.finisar.com/roadms-wavelength-management/10wsaaxxfl13>

²Product Code: EWP-AA-104-96F-ZZ-L <https://www.finisar.com/roadms-wavelength-management/ewp-aa-010x-96f-zz-l>

TABLE I: Lightpath characteristics before (top) and after (bottom) the introduction of L_5 . The listed channels are represented by the central frequency.

| | No. Channels | Physical Path | First Channel | Last Channel |
|-------|--------------|---------------|---------------|--------------|
| L_1 | 13 | p_2 | 192.8 THz | 194.0 THz |
| L_2 | 20 | p_2 | 194.1 THz | 196.0 THz |
| L_3 | 20 | p_1 | 192.8 THz | 194.7 THz |
| L_4 | 13 | p_1 | 194.8 THz | 196.0 THz |
| L_1 | 13 | p_1 | 193.5 THz | 194.7 THz |
| L_2 | 20 | p_2 | 194.1 THz | 196.0 THz |
| L_3 | 20 | p_2 | 192.1 THz | 194.0 THz |
| L_4 | 13 | p_1 | 194.8 THz | 196.0 THz |
| L_5 | 13 | p_1 | 192.2 THz | 193.4 THz |

the metropolitan optical network test-bed. Both tests consist of configuring the network to present an initial state and after it requiring the establishment of a new lightpath.

In the first experiment, the SDN controller is configured to sequentially send commands corresponding to *setup* and *tear-down* operations for each individual lightpath, according to the ASY approach. By contrast, in the second experiment, the SDN controller is configured to send only one command for each piece of equipment, reconfiguring all the lightpaths simultaneously, according to the TSO approach.

During the tests, a set of lightpaths L_n similar to those shown in Fig. 1 and Fig. 2 are defined, although, the branched topology is replaced by a plain one, with all lightpaths starting at node 1 for simplicity. The set of lightpaths are routed in the test-bed though two link-disjoint physical paths composed by the outermost nodes of the test-bed. In particular, as shown in Fig. 7, p_1 traverses nodes 1, 3 and 4; and p_2 traverses nodes 1, 2 and 4. Table I shows detailed information of each lightpath.

Note that when the DWDM 80-channel comb is launched into the network, the WSS at the first ROADM is used to filter undesired (interleaved) channels in order to generate a 40-channel scenario. This spacing is used to observe the noise power, thus the OSNR can be precisely estimated.

In the first experiment, the sequence of the SDN controller actions start at six different moments (likewise Fig. 3a):

- t_0 – establish initial state
- t_1 – tear-down L_3
- t_2 – tear-down L_1
- t_3 – setup L_1
- t_4 – setup L_3
- t_5 – setup L_5

On the other hand, in the second experiment, the sequence of the SDN controller actions start at two different moments (likewise Fig. 3b):

- t_0 – establish initial state
- t_1 – reroute lightpaths

After each action of the SDN controller, the optical spectra and powers for all nodes of the network are measured with an optical spectrum analyzer. The average OSNR and spectrum tilt (maximum difference of power among all channels) are also calculated at the last node of the physical paths. Since the first node of the path is used to select the input channels, the acquisition is performed after the WSS of this node, and

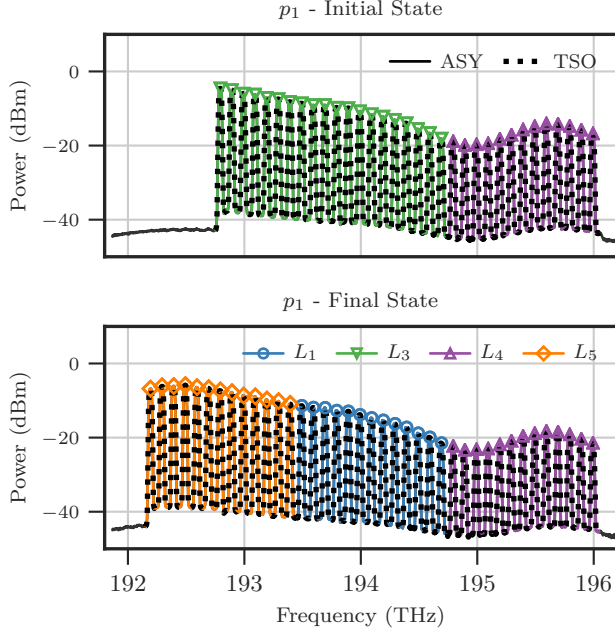


Fig. 8: Optical spectrum of the received signal at the last node of p_1 , before (top) and after (bottom) the introduction of L_5 for both techniques.

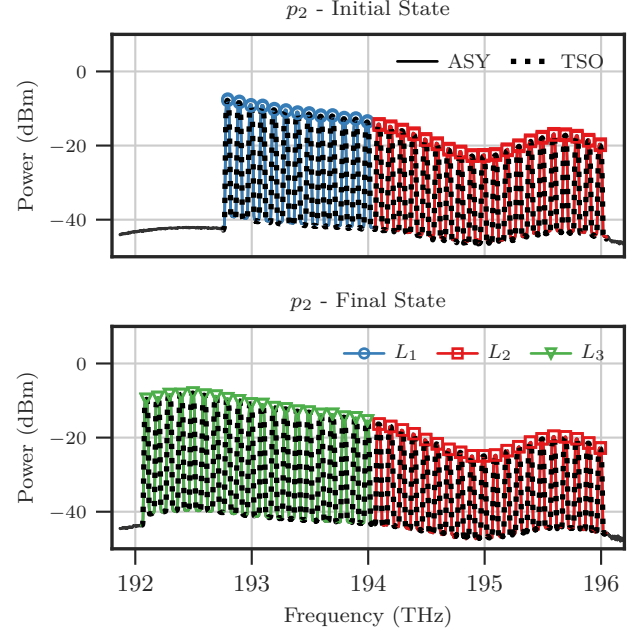


Fig. 9: Optical spectrum of the received signal at the last node of p_2 , before (top) and after (bottom) the introduction of L_5 for both techniques.

due to the node architecture, the measured power corresponds to $3/40$ of the WSS output power. For the other nodes, the acquisition is performed before the WSS, and due to the node architecture the measured power corresponds to $1/6$ of the amplifier output power. Therefore, different power levels between the first ROADMs and the subsequent ones are expected due to the different monitoring points inside the B&S architecture. Finally, it is worth mentioning that the attenuation performed at the WSSs is only applied to route the channel signals across the network, and is not applied to equalize each individual signal power. This choice is meant to better explore the physical layer implications in terms of power tilt across the C-band, and enables us to properly focus on the performance of the TSO-based approach against the traditional asynchronous technique. Future works may combine the current proposal in simultaneous operation with equalization techniques.

C. Experimental results and discussion

Figs. 8 and 9 show the optical spectrum of the signal received at the last node of each optical path, for both approaches in the initial and final states. In all charts, the curve for the TSO-based approach virtually overlaps the curve for the ASY technique. This result was already expected, since the channel configuration is the same, regardless of the technique, before and after the rerouting procedure. Interestingly, the optical power for the individual channels changes after the techniques are applied, as noticeable in the spectral region around 195 THz. These changes are a consequence of the non-linear dynamic behavior of the optical amplifiers whose gain profile depends on the input spectrum shape as a whole, but not only on the input power. A power tilt variation between

initial and final states can be observed (but not between the two approaches), since no flattening technique is used neither in the amplifiers nor in the WSSs, and this power tilt also changes after the introduction of the lightpath L_5 .

The impression that the chosen technique do not impact in the system performance in terms of signal quality, as suggested by the previous figures, is quantized by Table II, where performance indicators for the final state of the network are compared. The indicators for both techniques are hardly distinguishable.

Fig. 10 illustrates the changes in the optical power for all nodes, after each action of the SDN controller (here represented by the aforementioned time instants t_n). The optical power measured in the first node is one order of magnitude (in dB) lower than the other nodes because it is acquired in a different monitoring point, with a different split ratio as previously mentioned. As the total number of optical channels increase with the introduction of L_5 and not all the optical amplifiers are operating under saturation condition, an overall power increasing is experienced between the initial

TABLE II: Comparison of the two methodologies showcasing total power, average channel OSNR and spectrum tilt measured at the final node of the physical paths after the rerouting procedure.

| | ASY | | TSO | |
|-------------|-------|-------|-------|-------|
| | p_1 | p_2 | p_1 | p_2 |
| Power (dBm) | 4.66 | 2.81 | 4.62 | 2.80 |
| OSNR (dB) | 28.11 | 27.00 | 28.11 | 26.98 |
| Tilt (dB) | 17.44 | 16.95 | 17.47 | 16.96 |

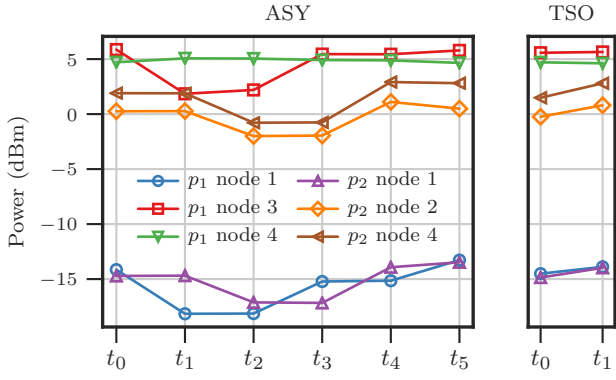


Fig. 10: Power fluctuations in each node of the test-bed during the rearrangements for both techniques.

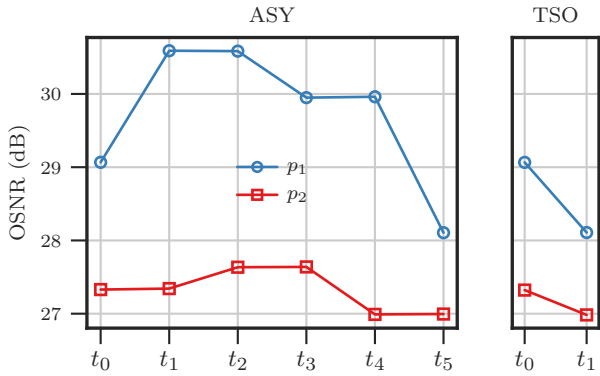


Fig. 11: Average OSNR variation during the rearrangements for both techniques.

and final states of the experiments. Moreover, during the first experiment, the optical power initially decreases in the first node, due to the two consecutive *tear-down* operations, but raises again with the *setup* operations. The curves for subsequent nodes follow this shape, with the exception of node 4 for p_1 , clearly due to a saturated amplifier.

Finally, Fig. 11 illustrates the changes in the OSNR of the received signal in the last node after the actions of the SDN controller. In a contrary way to the power behavior, the overall OSNR trend decreases despite of the intermediary increase in the first experiment. This is also a result of the non-linear dynamic behavior of the amplifier, because with low total input power (i.e., low number of channels) its performance in terms of OSNR improves.

VI. CONCLUSIONS

This paper reviewed our recent proposal time-synchronized operations (TSO) in software-defined elastic optical networks. In particular, we employed TSO to minimize disruption time during lightpath reassignment in EON and we discussed the SDN implementation details with NETCONF and OpenFlow exploiting their specific time-extensions. Then, we analytically elaborated that a joint combination of synchronization and bundling operations provides benefits in terms of minimizing

the lightpath disruption when swapping is required. Specifically, the TSO-based approaches OF and IA-NC outperform the ASY and N-NC implementations.

Subsequently, as mentioned in [1], here we extended our prior work with an experimental validation of our TSO-based proposal in a five-node metropolitan optical network test-bed. We developed an SDN application that emulates the operations required by the ASY approach to compare its performance against the TSO-based approach. Our reported results validated the convenience of the TSO-based approach against a traditional ASY technique given its reduction of disruption time while both techniques exhibited close network performance indicators (e.g., OSNR, power budget, spectrum tilt) after preforming the lightpath swapping.

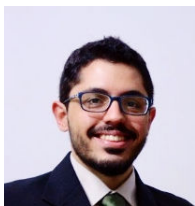
ACKNOWLEDGMENT

This work was partially funded by the Brazilian Ministry of Communications (FUNTTEL/FINEP) under the project 100 GETH. Miquel Garrich thanks CNPq (grant 312047/2015-0).

REFERENCES

- [1] A. S. Muqaddas, M. Garrich, P. Giaccone, A. Bianco "Exploiting Time-Synchronized Operations in Software-defined Elastic Optical Networks," *Optical Fiber Communication Conference*, Los Angeles, USA, 2017.
- [2] J. P. Fernandez-Palacios, V. López, B. Cruz and O. G. de Dios, "Elastic optical networking: An operators perspective," *Proceedings of European Conference on Optical Communication (ECOC)*, 2014, pp. 1-3.
- [3] A. Lord, P. Wright and A. Mitra, "Core Networks in the Flexgrid Era," *Journal of Lightwave Technology*, vol. 33, no. 5, pp. 1126-1135, March 2015.
- [4] J. Zhang, Y. Ji, M. Song, Y. Zhao, X. Yu, J. Zhang and B. Mukherjee et al., "Dynamic Traffic Grooming in Sliceable Bandwidth-Variable Transponder-Enabled Elastic Optical Networks," *Journal of Lightwave Technology*, vol. 33, no. 1, pp. 183-191, Jan 2015.
- [5] ITU-T Recommendation "G.694.1: Spectral grids for WDM applications: DWDM frequency grid" Feb. 2012. Available at <https://www.itu.int/rec/T-REC-G.964.1/en>
- [6] J. L. Vizcaíno, Y. Ye, V. López, F. Jiménez, R. Duque, and P. M. Krummrich, "Cost evaluation for flexible-grid optical networks," *GlobeCom Workshops*, pp. 358-363, Anaheim, California, USA, December 2012.
- [7] X. Yu, M. Tornatore, M. Xia, Y. Zhao, J. Zhang, and B. Mukherjee, "Brown-field migration from fixed grid to flexible grid in optical networks," *Optical Fiber Communication Conference*, pp. W11-4, Los Angeles, California, USA, 2015.
- [8] Blair, J. Marsella, T. Szyrkowicz, A. Autenrieth, C. Liou, A. Sasdasivarao, S. Syed, J. Sun, B. Rao, F. Zhang, and J. Fernández-Palacios, "Demonstration of SDN orchestration in optical multi-vendor scenarios," *Optical Fiber Communication Conference*, Los Angeles, California, USA, March 2015.
- [9] M. Cantono, R. Gaudino, and V. Curri, "Potentialities and Criticalities of Flexible-Rate Transponders in DWDM Networks: A Statistical Approach," *Journal of Optical Communications and Networking*, vol. 8, no. 7, pp. A76-A85, 2016.
- [10] A. Giorgetti, F. Paolucci, F. Cugini and P. Castoldi, "Dynamic restoration with GMPLS and SDN control plane in elastic optical networks [Invited]" *Journal of Optical Communications and Networking*, vol. 8, no. 7, pp. A174-A182, 2015.
- [11] D. Kreutz, F. M. Ramos, P. E. Verissimo, C. E. Rothenberg, S. Azodolmoly, and S. Uhlig, "Software-defined networking: A comprehensive survey," *Proceedings of the IEEE*, vol. 103, no. 1, pp. 14-76, 2015.
- [12] YANG IETF NETCONF Data Modeling Language Working Group, Oct. 2010. Available: <https://tools.ietf.org/html/rfc6020>
- [13] M. Dallaglio, N. Sambo, J. Akhtar, F. Cugini, and P. Castoldi, "YANG Model and NETCONF Protocol for Control and Management of Elastic Optical Networks," *Optical Fiber Communication Conference*, Anaheim, California, USA, 2016.
- [14] J. Akhtar, "YANG modeling of network elements for the management and monitoring of Elastic Optical Networks," *IEEE International Conference on Telecommunications and Photonics*, pp. 1-5, Dhaka, Bangladesh, 2015.

- [15] M. Dallaglio, N. Sambo, F. Cugini, and P. Castoldi, "Management of sliceable transponder with NETCONF and YANG," *Optical Network Design and Modeling*, Cartagena, Spain, 2016.
- [16] M. Dallaglio, N. Sambo, F. Cugini, and P. Castoldi, "Pre-programming resilience schemes upon failure through NETCONF and YANG," *Optical Fiber Communication Conference*, Los Angeles, USA, 2017.
- [17] The Open ROADM Multi-Source Agreement, available at: <http://www.openroadm.org/>
- [18] B. C. Chatterjee, N. Sarma and E. Oki, "Routing and Spectrum Allocation in Elastic Optical Networks: A Tutorial," *IEEE Communications Surveys & Tutorials*, vol. 17, no. 3, pp. 1776-1800, 2015.
- [19] F. Cugini, F. Paolucci, G. Meloni, G. Berrettini, M. Secondini, F. Fresi, N. Sambo, L. Poti and P. Castoldi, "Push-Pull Defragmentation Without Traffic Disruption in Flexible Grid Optical Networks," *Journal of Lightwave Technology*, vol. 31, no. 1, pp. 125-133, Jan 2013.
- [20] R. Proietti, C. Qin, B. Guan, Y. Yin, R. P. Scott, R. Yu, and S. J. B. Yoo, "Rapid and complete hitless defragmentation method using a coherent RX LO with fast wavelength tracking in elastic optical networks," *Optics Express*, vol. 20, no. 24, pp. 26958-26968, 2012.
- [21] R. Wang and B. Mukherjee, "Provisioning in Elastic Optical Networks with Non-Disruptive Defragmentation," *Journal of Lightwave Technology*, vol. 31, no. 15, pp. 2491-2500, Aug 2013.
- [22] S. Ba, B. C. Chatterjee, S. Okamoto, N. Yamanaka, A. Fumagalli and E. Oki, "Route partitioning scheme for elastic optical networks with hitless defragmentation," *Journal of Optical Communications and Networking*, vol. 8, no. 6, pp. 356-370, June 2016.
- [23] T. Mizrahi and Y. Moses, "Time4: Time for SDN," *IEEE Transactions on Network and Service Management*, vol. 13, no. 3, pp. 433-446, Sept. 2016.
- [24] P. Megyesi, A. Botta, G. Aceto, A. Pescapé, and S. Molnár, Challenges and solution for measuring available bandwidth in software defined networks, *Computer Communications*, v. 99, pp. 48-61, Feb. 2017.
- [25] Y. Li, N. Hua, Y. Song, S. Li, and X. Zheng, Fast Lightpath Hopping Enabled by Time Synchronization for Optical Network Security, *IEEE Communication Letters*, v. 20, n. 1, pp. 101-104, Jan. 2015.
- [26] D. Awduche, L. Berger, D. Gan, T. Li, V. Srinivasan, G. Swallow, "RSVP-TE: Extensions to RSVP for LSP Tunnels," IETF RFC 3209, Dec. 2001.
- [27] T. Mizrahi and Y. Moses, "Time Capability in NETCONF", IETF RFC 7758, Feb 2016.
- [28] M. Garrich, A. Bravalheri, M. Magalhães, M. Svolsenski, X. Wang, Y. Fei, A. Fumagalli, D. Careglio, J. Solé-Pareta, J. Oliveira, "Demonstration of dynamic traffic allocation in an SDN-enabled metropolitan optical network test-bed," *International Conference on Optical Network Design and Modeling*, Cartagena, Spain, 2016.
- [29] OpenFlow Switch Specification, Version 1.5.2 (Wire Protocol 0x06), ONF, 2015.
- [30] T. Mizrahi and Y. Moses, "ReversePTP: a software defined networking approach to clock synchronization," *Hot topics in software defined networking (HotSDN '14)*, pp. 203-204, New York, NY, USA.
- [31] A. Shakeri et al., "Estimating the effect of Wavelength Selective Switch latency on optical flow switching performance," *International Conference on High Performance Switching and Routing (HPSR)*, Campinas, SP, Brazil, 2017, pp. 1-6.
- [32] Calient (available at <http://www.calient.net/>) and Polatis (available at <http://www.polatis.com/>) MEMS-based optical switches.



Anderson Cleyton Bravalheri received his Bachelor degree in Electrical Engineering and his Master degree in Electrical Engineering (Telecommunications and Telematics) from University of Campinas (UNICAMP), Brazil in 2011 and 2016 respectively. From 2011 to 2017, he was a telecommunication researcher at CPqD where he had the opportunity to work on a wide variety of technical projects covering from control of optical components and firmware development up to SDN applications for optical networks. Currently, he is a Research Associate at

University of Bristol, UK, and his interests include Optical Communications, Fuzzy Control, Machine Learning, Distributed Systems, Graph Theory, Software Defined Networks, Network Function Virtualization, Service Function Chaining and Network and Function Management and Orchestration.



Miquel Garrich Alabarcé is Telecommunications Engineer by Universitat Politècnica de Catalunya, Spain (2009) and PhD by Politecnico di Torino, Italy (2013). As PhD candidate, he did a visiting researcher stage at the High Performance Networks group, University of Essex, UK. During 5 years, he was senior researcher in the optical technologies division at CPqD, Campinas, Brazil, where he coordinated several R&D activities and technological transferences to the (Brazilian) industry in the optical networks team including amplifiers, ROADMs, and SDN. In 2017, he revisited Politecnico di Torino as junior lecturer during one year. He recently obtained a H2020 Marie Skłodowska-Curie individual fellowship (2018-2020) to be fulfilled at Universidad Politécnica de Cartagena, Spain, in collaboration with Telefónica Investigación y Desarrollo, Madrid, Spain.



Abubakar Siddique Muqaddas received the B.E. in Electrical (Telecommunications) Engineering from NUST, Rawalpindi, Pakistan and M.Sc. in Telecommunications Engineering from Politecnico di Torino, Italy, in 2011 and 2015 respectively. Currently he is a Ph.D. candidate in the Electrical, Electronics and Telecommunications Engineering program in Politecnico di Torino. He is a Cisco Certified Network Associate (CCNA) and a Cisco Certified Network Professional (CCNP). His current interests are in assessing distributed SDN controller

architectures, software-defined optical network operations and management of state in SDN.



Paolo Giaccone received the Dr.Ing. and Ph.D. degrees in telecommunications engineering from the Politecnico di Torino, Torino, Italy, in 1998 and 2001, respectively. He is currently an Associate Professor in the Department of Electronics, Politecnico di Torino. During the summer of 1998, he was with the High Speed Networks Research Group, Lucent Technology-Bell Labs, Holmdel, NJ. During 2000-2001 and in 2002 he was with the Information Systems Networking Lab, Electrical Engineering Dept., Stanford University, Stanford, CA. His main area of

interest is the design of network algorithms, in particular for the control of SDN networks, of optical networks and of cloud computing systems.



Andrea Bianco is Full Professor and Department Head of the Dipartimento di Elettronica e Telecomunicazioni di Politecnico di Torino, Italy. He has coauthored over 200 papers published in international journals and presented in leading international conferences in the area of telecommunication networks. He is Area Editor for the IEEE JLT (Journal of Lightwave Technology) and of the Elsevier Computer Communications journal. His current research interests are in the fields of protocols and architectures of all-optical networks, switch architectures for

high-speed networks, SDN networks and software routers. Andrea Bianco is an IEEE Senior Member.